Research Article | Vol. 32, No. 11 / 20 May 2024 / Optics Express 18909
Optics EXPRESS

Easily variable and scalable terahertz pulse source based on tilted-pulse-front pumped semiconductors

GERGŐ KRIZSÁN,[1,2,3,*] ZOLTÁN TIBAI,[1] GYÖRGY TÓTH,[1] JÁNOS HEBLING,[1,2] AND LÁSZLÓ PÁLFALVI[1,3]

[1]Institute of Physics, University of Pécs, Pécs, Hungary
[2]Szentágothai Research Centre, University of Pécs, Pécs, Hungary
[3]HUN-REN–PTE High-Field Terahertz Research Group, Pécs, Hungary
[*]krizsan@fizika.ttk.pte.hu

Abstract: A new type of terahertz source containing only two optical elements - a volume phase holographic grating, and a semiconductor nonlinear slab - is proposed. The setup does not require any microstructuring, has only one diffraction order, and can be scaled to large pump sizes without any principal limitations. Furthermore, it can be easily adapted to different pump wavelengths and THz phase-matching frequencies. The Fresnel loss at the boundary of the materials can be significant at conventional pump polarizations (s-pol), but a single-layer anti-reflection (AR) coating can reduce it. Pumping such a setup with polarization in the dispersion plane (p-pol, TM mode) can reduce the effective nonlinear polarization and consequently the terahertz generation efficiency. However, in the absence of AR coating, this reduction is overcompensated by the reduced Fresnel loss.

1. Introduction

Intense nearly single-cycle terahertz (THz) pulses can be used in materials science [1] and for the acceleration of free electrons and protons [2–6]. Optical rectification of femtosecond laser pulses has become the most efficient source of intense THz pulses in the low- (about 0.1–2 THz) [7] and mid-frequency (about 2–20 THz) part of the THz spectrum [8]. Conventional tilted-pulse-front pumping (TPFP) of $LiNbO_3$ (LN) prism has been providing the highest THz pulse energies and efficiencies in the low-frequency part of the THz spectrum [9], making it particularly advantageous for particle acceleration. However, the prism shape of the LN crystal and the imaging used in these setups cause substantial limitations on THz energy scalability and beam quality [10]. In recent years, considerable efforts have been dedicated to mitigating or entirely eliminating these limitations [10].

It has been recently demonstrated that semiconductor nonlinear materials offer a promising alternative with scalability to the highest THz pulse energies and field strengths [11,12], also enabling the construction of monolithic contact-grating (CG) sources [12–14]. Semiconductor materials need to be pumped at an infrared wavelength sufficiently long to suppress two- and three-photon absorption, to avoid the associated free-carrier absorption in the THz range [15]. Typically, TPFP is needed in this case for phase (velocity) matching [15–17], but the pulse-front-tilt (PFT) angle - and correspondingly the angular dispersion - is significantly smaller (~20°-25°) compared to the LN sources.

In the case of plan-parallel CG semiconductor THz sources, the strongest limitation factor arises from the co-propagating ±1 diffraction orders. Their interference limits on a lower value the efficiently usable pump intensity and correspondingly, the pump-to-THz conversion efficiency.

#519853 https://doi.org/10.1364/OE.519853
Journal © 2024 Received 24 Jan 2024; revised 12 Mar 2024; accepted 20 Mar 2024; published 8 May 2024

Optics EXPRESS

Recently, semiconductor-based THz pulse sources were suggested [18], where the microstructuring of the front (NLES) or the back surface (RNLS) of the semiconductor is still needed, but only one diffraction order has high diffraction efficiency.

In the present paper, we introduce a simple and compact setup, which includes the advantages of the previous designs (no imaging, energy and size scalability, one diffraction order) but do not require the microstructuring of the semiconductor slab's surfaces. Furthermore, it is easily adaptable to different pump wavelengths and phase-matched THz frequencies. For a direct comparison with previously introduced setups [15,17], we selected GaP as the semiconductor nonlinear material, a 1.8 μm pump wavelength, and a 3 THz phase-matching frequency. In this case, the necessary PFT angle is 22.5°.

2. Proposed setup

The proposed THz pulse source setup is shown in Fig. 1. It is based on optical rectification in GaP using the tilted-pulse-front technique and contains only two optical elements: a volume phase holographic grating (VPHG), which introduces the necessary PFT, and a plan-parallel semiconductor slab. Between the two, a refractive index matching liquid (RIML) is used for efficient in-coupling. We call this combination of VPHG and semiconductor nonlinear slab (SNLS) VPHG-SNLS.

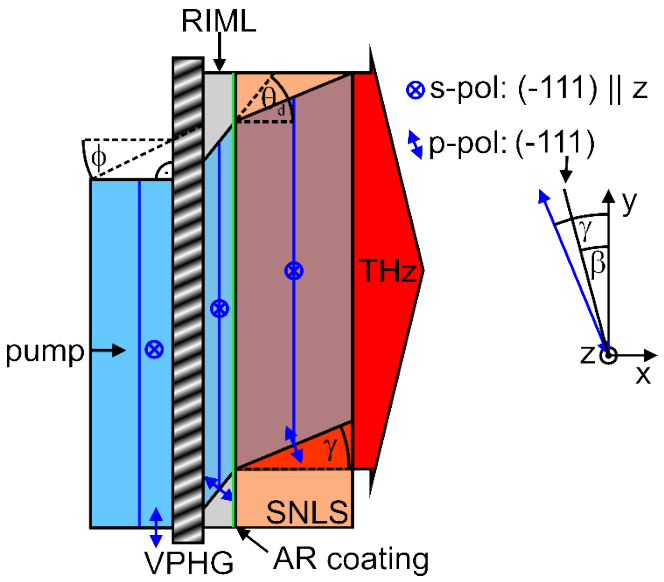

Fig. 1. Schematic drawing of the VPHG-SNLS THz source. If the pump has s-pol the (−111) crystal axis should be parallel with the z axis and an optional AR coating can be applied to the SNLS front surface to reduce the Fresnel loss. In case of p-pol the (−111) axis should make a β angle -which is about the 2/3 of the γ angle - with the y axis (see Section 3 for more detail).

The pump beam has a normal incidence on the VPHG. After the diffraction, the pump beam propagates through the RIML and reaches the plan-parallel SNLS at a θ_d incidence angle as seen in Fig. 1. The angle of refraction in the SNLS has to be equal to the PFT angle (γ) required by the velocity matching condition. This can be reached by the proper choice of the d grating period of the VPHG according to:

$$\sin(\gamma) = \frac{\lambda_0}{nd}, \tag{1}$$

Optics EXPRESS

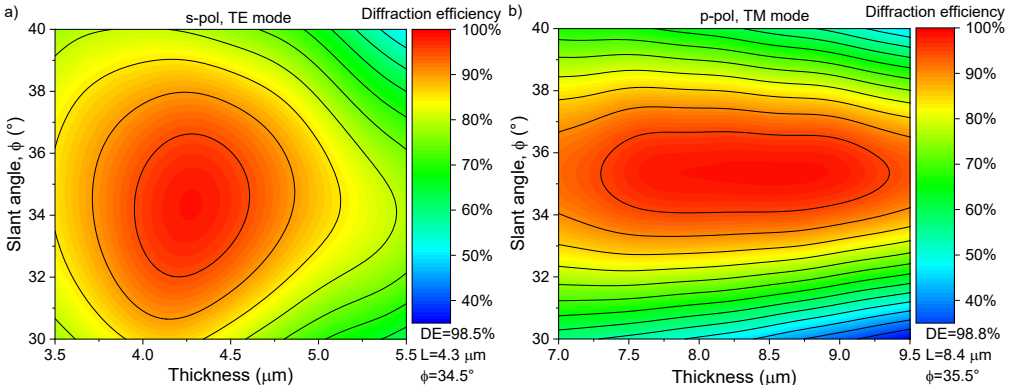

Fig. 2. VPHG diffraction efficiency simulations for the VPHG-SNLS THz sources in the case of s- (a) and p-polarizations (b).

where λ_0 is the pump wavelength in vacuum and n is the refractive index of the SNLS. The THz pulse generated in such a way travels along the x direction and leaves the SNLS perpendicularly to its back surface.

VPHGs can have high diffraction efficiency at normal incidence if the planes of constant refractive index are appropriately tilted (slanted), as indicated in Fig. 1. For manufacturing purposes this slant angle should not be much greater than 35°. At higher angles, the planes of constant refractive index can become curved, which will result in a smaller diffraction efficiency. As previously in Ref. [19] we supposed dichromated gelatin (DCG) as the VPHG photosensitive material [20], which is sealed in between BK7 windows to support it and protect it from dust and humidity [21].

For RIML the most obvious choice is a RIML having the refractive index of BK7 glass, which is commercially available and safe to use down to ~ −40 C° temperature and eliminates the Fresnel loss between the VPHG window and the RIML. To achieve even lower temperatures or to further reduce the overall Fresnel loss (including the loss at the RIML – SNLS surface, which is relatively high) other liquids with higher refractive index and with a lower freezing point can be used e.g., CS_2 or even nanofluids [22] based on CS_2 [18]. It is also possible to reduce the Fresnel loss between the BK7 RIML and SNLS by applying an anti-reflection (AR) coating on the SNLS front surface. In the case of GaP SNLS, with a single layer TiO_2 AR coating the loss can be decreased to <4%. Another possibility to decrease significantly the Fresnel loss is using a pump with polarization in the dispersion plane (p-pol) since the incident angle at the RIML and SNLS boundary is close to the Brewster angle. This way the Fresnel loss can be reduced from ~30 to ~5%, however, the SNLS has to be oriented differently, which can lead to a reduced effective nonlinear optical coefficient and THz generation efficiency. This will be discussed in detail in Section 3.

The proposed setup can be easily adapted to different pump wavelengths and THz phase-matching frequencies, simply by changing the VPHG. The designed VPHGs below can have high diffraction efficiency (>80%) in a ~220 (~120) nm wavelength range in case of s-pol (p-pol). So, in case of different pump wavelength the same VPHG may be used, with somewhat lower diffraction efficiency and the generated THz frequency will shift too. A ± 100 nm shift of the pump wavelength (from 1.8 μm) results a ~±1.3° PFT angle change (from 22.5°), which shifts the phase matching angle by ~1 THz (from 3 THz). We would like to note that the VPHG-SNLS setup is feasible up to 2.5 μm pump wavelength, where the absorption of the DCG becomes significant [23].

Optics EXPRESS

In Fig. 2 the numerical simulation (COMSOL) results of the VPHG diffraction efficiency with a line density of 647 line/mm can be seen for the two polarization states. For the simulation, we supposed an average refractive index value of the DCG $n_{DCG} = 1.35$ and an index modulation of $\Delta n_{DCG} = 0.15$. As it is expected the optimum thickness of the DCG is almost two times larger for the p-polarization, and the predicted diffraction efficiency maxima are exceptionally high for both gratings. The optimal slant angle is near the well-feasible limit in both cases, but smaller for the s-polarization. The VPHG for s-polarization is less sensitive to the slant angle variation, while the VPHG for p-polarization is less sensitive to the thickness variation.

Simulation results on THz pulse generation for such a setup can be found in [18] for single cycle, and in [24] for multicycle THz generation.

3. Pump polarization in the dispersion plane

For optical rectification (THz generation) the d_{ijk} second-order nonlinear optical tensor element has to be calculated from the r_{ijk} electro-optical tensor element by the following equation [16]:

$$d_{ijk} = -\frac{n_{SNLS}^4 r_{ijk}}{4}, \tag{2}$$

where n_{SNLS} is the refractive index of the SNLS at the pump wavelength. For zinc-blende type crystals, like GaP, there are three nonvanishing contracted matrix elements and those have the same values ($r_{14} = 0.97\frac{pm}{V}$) [25]. The matrix is:

$$\boldsymbol{d} = \begin{bmatrix} 0 & 0 & 0 & d_{14} & 0 & 0 \\ 0 & 0 & 0 & 0 & d_{25} & 0 \\ 0 & 0 & 0 & 0 & 0 & d_{36} \end{bmatrix}, \tag{3}$$

where $d_{14} = d_{123}$, d_{132}; $d_{25} = d_{231}, d_{213}$; $d_{36} = d_{312}$, d_{321}. To calculate the nonlinear polarization for the p-polarization case, with pump polarization restricted to the dispersion plane (xy), a possible way is to rotate the SNLS. The $\boldsymbol{R}$ rotation matrix is the following:

$$\boldsymbol{R} = \begin{bmatrix} \mathrm{c}(\alpha)\mathrm{c}(\beta) - \mathrm{c}(\theta)\mathrm{s}(\alpha)\mathrm{s}(\beta) & -\mathrm{c}(\beta)\mathrm{s}(\alpha) - \mathrm{c}(\theta)\mathrm{c}(\alpha)\mathrm{s}(\beta) & \mathrm{s}(\beta)\mathrm{s}(\theta) \\ \mathrm{c}(\alpha)\mathrm{s}(\beta) + \mathrm{c}(\beta)\mathrm{c}(\theta)\mathrm{s}(\alpha\phi) & \mathrm{c}(\alpha)\mathrm{c}(\theta)\mathrm{c}(\beta) - \mathrm{s}(\alpha)\mathrm{s}(\beta) & -\mathrm{c}(\beta)\mathrm{s}(\theta) \\ \mathrm{s}(\theta)\mathrm{s}(\alpha) & \mathrm{c}(\alpha)\mathrm{s}(\theta) & \mathrm{c}(\theta) \end{bmatrix}, \tag{4}$$

where c and s are abbreviations for the cosine and sinus functions, α, θ, and β are the rotation angles around the z, x, and again the z-axis, respectively. After the rotation, the transformed d''_{ijk} tensor elements (represented in the xyz coordinate system) can be determined as:

$$d''_{ijk} = \sum_{IJK} R_{iI} R_{jJ} R_{kK} d_{IJK}. \tag{5}$$

The i^{th} component of the nonlinear polarization vector can be determined by:

$$P_i^{NL} = 2\epsilon_0 \sum_{jk} d''_{ijk} E_j E_k, \tag{6}$$

where E_j and E_k are the electric field components of the pump. The electric field of the generated THz pulse will be proportional to $\boldsymbol{P^{NL}}$, while its intensity to $\boldsymbol{P^{NL^2}} = \sum_i (P_i^{NL})^2$. So, in order to maximize the THz pulse generation efficiency the $\boldsymbol{P^{NL^2}}$ - calculated from Eqs. (2) – (6) - has to be maximized by the optimal choice of the α, θ, and β angles.

Optics EXPRESS

In case of zinc-blende type crystals the nonlinear polarization reaches maximum value if either the (−1 1 1) or the (1 −1 1) axis is parallel with the pump polarization. In order to check the validity of the computation trivial cases were investigated:

If the pump polarization is parallel to the z axis, i.e., $\boldsymbol{E} = E_0 \begin{bmatrix} 0 \\ 0 \\ 1 \end{bmatrix}$, only the z component of $\boldsymbol{P^{NL}}$ is non zero, and $\boldsymbol{P^{NL^2}}$ has a maximum if $\alpha = -\pi/4$, $\theta = \arcsin\left(\sqrt{2/3}\right)$, and β is arbitrary. Its maximum value is $\boldsymbol{P^{NL^2}} = \frac{16}{3}\epsilon_0^2 d_{14}^2 E_0^4$ [26] corresponding to the conventionally used case when the polarization is perpendicular to the dispersion plane (s-pol), and it is parallel to the (−1 1 1) and the z axis in Fig. 1.

Similarly to the previous case, if the pump polarization is parallel to the y (x) axis, i.e., $\boldsymbol{E} = E_0 \begin{bmatrix} 0 \\ 1 \\ 0 \end{bmatrix}$ ($\boldsymbol{E} = E_0 \begin{bmatrix} 1 \\ 0 \\ 0 \end{bmatrix}$), $\boldsymbol{P^{NL}}$ (and the THz field as well) has only y (x) nonzero component, and $\boldsymbol{P^{NL^2}}$ has a maximum if $\alpha = -\pi/4$, $\theta = -\arcsin\left(\sqrt{\frac{1}{3}}\right)$, $\beta = 0$ ($\alpha = -\frac{\pi}{4}$, $\theta = -\arcsin\left(\sqrt{\frac{1}{3}}\right)$, $\beta = -\pi/2$) as expected.

In the case of TPFP pumping when the pump polarization is in the dispersion plane with $\boldsymbol{E} = E_0 \begin{bmatrix} -\sin(\gamma) \\ \cos(\gamma) \\ 0 \end{bmatrix}$, the THz propagation direction is along the x-axis as it can be seen in Fig. 1, so the x component of the nonlinear polarization cannot contribute to the generated THz field, therefore $P_y^{NL^2} + P_z^{NL^2}$ has to be maximized. This holds, if $\alpha = -\mathrm{Pi}/4$, $\theta = -\arcsin\left(\sqrt{1/3}\right)$ (similarly as for the two specific cases discussed above) and β is about 2/3 of the PFT (γ) angle. Here, it is worth to introduce the square of the effective and normalized nonlinear polarization, which (in the case of TPFP) can be given by the following equation:

$$P_{eff}^{NL^2} = \frac{P_y^{NL^2} + P_z^{NL^2}}{\epsilon_0^2 d_{14}^2 E_0^4} \,. \tag{7}$$

In Fig. 3 the β angle - which is the second rotation angle around the z-axis, and the angle between the (−1 1 1) crystal axis and the y-axis (see Fig. 1) - and the corresponding value of $P_{eff}^{NL^2}$ is plotted for the different PFT (γ) angles. This PFT angle interval corresponds to 1.7-2.2 μm pump wavelength and 1-4 THz phase-matching frequency intervals.

The ~5.07 $P_{eff}^{NL^2}$ value belonging to $\gamma = 22.5°$ is ~5% lower, than the 16/3 value belonging to the s-pol. According to numerical simulations (the model is described in Ref [17]) this ~5% decrease in $\boldsymbol{P^{NL^2}}$ (the optimal case for p-pol contrary to the case of s-pol) will decrease the THz generation efficiency by ~5% as expected. This is overcompensated by the ~22.4% efficiency gain due to the reduction of the Fresnel losses when p-pol is used instead of s-pol. This means that resultantly (taking into consideration both the Fresnel loss and the effective value of the nonlinear optical coefficient) the use of p-pol is more advantageous, if no AR coating can be applied to the SNLS surface.

In case of s-pol a conventionally oriented SNLS can be used, the VPHG can be manufactured a bit more easily, and it can be used efficiently in a bit larger wavelength range. With an AR coating

Optics EXPRESS

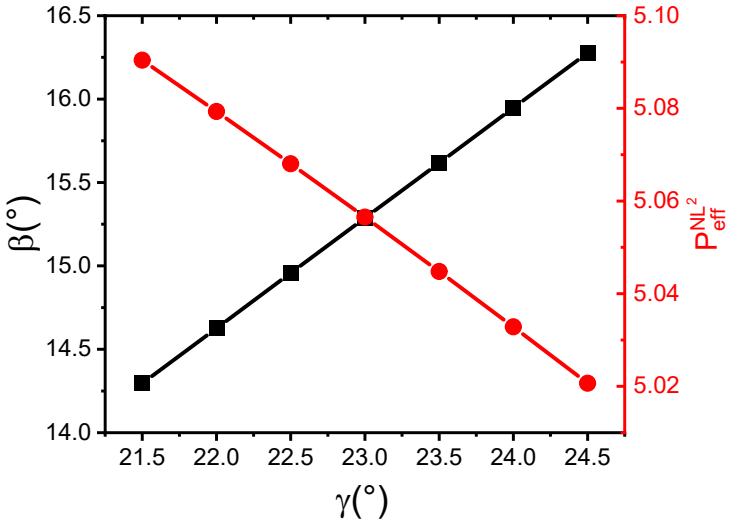

Fig. 3. The β angle (black squares), and the corresponding value of $P_{eff}^{NL^2}$ (red circles) vs. the γ PFT angle.

on the SNLS surface it has very similar or even lower Fresnel loss and therefore higher THz generation efficiency than the p-pol case. The effective and normalized nonlinear polarization and the Fresnel loss values are collected in Table 1 for the two polarization cases.

Table 1. The effective and normalized nonlinear polarization, and the reflection loss at the VPHG-SNLS boundary for the two polarization states.

polarization	$P_{eff}^{NL^2}$	Fresnel loss
s-pol	16/3	~25%
p-pol	~5.07	~2.6%

It is useful to mention two other special TPFP cases. If $\beta = \gamma$ the generated THz field will only have y component (even if $P_x^{NL^2} \neq 0$), and $P_y^{NL^2}$ will be significantly smaller and have a value of $\frac{16}{3}\cos^2(\gamma)\epsilon_0^2 d_{14}^2 E_0^4$. If $\beta = 0$, which could be a choice for the CG setup, where the ± 1 diffraction orders propagate together $P_{eff}^{NL^2}$ will be even smaller (~62% of the conventional value). Therefore, this method - when the pump polarization is in the dispersion plane - is not recommended for the CG setup, even if it can have higher diffraction efficiency in TM mode.

4. Conclusion

A new compact and scalable THz pulse source is proposed, which contains only two optical elements. A VPHG, which introduces the necessary PFT angle and a plan-parallel semiconductor slab. The setup is easily feasible since it does not require microstructuring. The only drawback of the setup is that the Fresnel loss between the RIML and SNLS can be relatively large. This can be decreased with a single-layer AR coating or by using a pump having polarization in the dispersion plane. The latter reduces the effective nonlinear polarization value and leads to reduced THz generation efficiency, but decreases the Fresnel loss too, which effect is more significant.

Optics EXPRESS

Funding. National Research, Development and Innovation Office (2018-1.2.1-NKP-2018-00009, 2018-1.2.1-NKP-2018-00010, OTKA K 23(147409), TKP2021-EGA-17).

Acknowledgments. Zoltán Tibai would like to thank the support of the János Bolyai Research Scholarship of the Hungarian Academy of Sciences.

Disclosures. The authors declare no conflicts of interest.

Data availability. The data supporting this study's findings are available within the article and from the corresponding author upon reasonable request.

References

1. P. Salén, M. Basini, S. Bonetti, *et al.*, "Matter manipulation with extreme terahertz light: Progress in the enabling THz technology," Phys. Rep. **836-837**, 1–74 (2019).
2. D. Zhang, A. Fallahi, M. Hemmer, *et al.*, "Segmented terahertz electron accelerator and manipulator (STEAM)," Nat. Photonics **12**(6), 336–342 (2018).
3. M. T. Hibberd, A. L. Healy, D. S. Lake, *et al.*, "Acceleration of relativistic beams using laser-generated terahertz pulses," Nat. Photonics **14**(12), 755–759 (2020).
4. H. Tang, L. Zhao, P. Zhu, *et al.*, "Stable and scalable multistage terahertz-driven particle accelerator," Phys. Rev. Lett. **127**(7), 074801 (2021).
5. E. Curry, S. Fabbri, J. Maxson, *et al.*, "Meter-scale terahertz-driven acceleration of a relativistic beam," Phys. Rev. Lett. **120**(9), 094801 (2018).
6. L. Pálfalvi, J. Fülöp, G. Tóth, *et al.*, "Evanescent-wave proton postaccelerator driven by intense THz pulse," Phys. Rev. ST Accel. Beams **17**(3), 031301 (2014).
7. S.-W. Huang, E. Granados, W. R. Huang, *et al.*, "High conversion efficiency, high energy terahertz pulses by optical rectification in cryogenically cooled lithium niobate," Opt. Lett. **38**(5), 796–798 (2013).
8. M. Shalaby and C. P. Hauri, "Demonstration of a low-frequency three-dimensional terahertz bullet with extreme brightness," Nat. Commun. **6**(1), 5976 (2015).
9. B. Zhang, Z. Ma, and J. Ma, "1.4-mJ High Energy Terahertz Radiation from Lithium Niobates," Laser Photonics Rev. **15**(3), 2000295 (2021).
10. G. Tóth, L. Pálfalvi, and S. Turnár, "Performance comparison of lithium-niobate-based extremely high-field single-cycle terahertz sources," Chin. Opt. Lett. **19**(11), 111902 (2021).
11. F. Blanchard, B. Schmidt, and X. Ropagnol, "Terahertz pulse generation from bulk GaAs by a tilted-pulse-front excitation at 1.8 μ m," Appl. Phys. Lett. **105**(24), 241106 (2014).
12. J. A. Fülöp, G. Polónyi, and B. Monoszlai, "Highly efficient scalable monolithic semiconductor terahertz pulse source," Optica **3**(10), 1075–1078 (2016).
13. W. Cui, K. M. Awan, R. Huber, *et al.*, "Broadband and High-Sensitivity Time-Resolved THz System Using Grating-Assisted Tilted-Pulse-Front Phase Matching," Adv. Opt. Mater. **10**(1), 2101136 (2022).
14. M. Bashirpour, W. Cui, A. Gamouras, *et al.*, "Scalable Fabrication of Nanogratings on GaP for Efficient Diffraction of Near-Infrared Pulses and Enhanced Terahertz Generation by Optical Rectification," Crystals **12**(5), 684 (2022).
15. N. M. Mbithi, G. Tóth, Z. Tibai, *et al.*, "Investigation of terahertz pulse generation in semiconductors pumped at long infrared wavelengths," J. Opt. Soc. Am. B **39**(10), 2684–2691 (2022).
16. J. Hebling, K.-L. Yeh, M. C. Hoffmann, *et al.*, "Generation of high-power terahertz pulses by tilted-pulse-front excitation and their application possibilities," J. Opt. Soc. Am. B **25**(7), B6–B19 (2008).
17. Gy. Tóth, Gy. Polónyi, and J. Hebling, "Tilted pulse front pumping techniques for efficient terahertz pulse generation," Light: Sci. Appl. **12**(1), 256 (2023).
18. Z. Tibai, G. Krizsán, G. Tóth, *et al.*, "Scalable microstructured semiconductor THz pulse sources," Opt. Express **30**(25), 45246–45258 (2022).
19. G. Krizsán, Z. Tibai, and G. Tóth, "Uniformly scalable lithium niobate THz pulse source in transmission geometry," Opt. Express **30**(3), 4434–4443 (2022).
20. L. D. Dickson, R. D. Rallison, and B. H. Yung, "Holographic polarization-separation elements," Appl. Opt. **33**(23), 5378–5385 (1994).
21. S. C. Barden, J. A. Arns, and W. S. Colburn, "Volume-Phase Holographic Gratings and the Efficiency of Three Simple Volume-Phase Holographic Gratings," Publ. Astron. Soc Pac. **112**(772), 809–820 (2000).
22. M. Trikeriotis, R. Rodriguez, and M. F. Zettel, "High refractive index nanoparticle fluids for 193-nm immersion lithography," in *Advances in Resist Materials and Processing Technology XXVI* (International Society for Optics and Photonics, 2009), p. 72732A.
23. N. Ebizuka, K. Ichiyama, and T. Yamada, "Cryogenic Volume-Phase Holographic Grisms for MOIRCS," Publ. Astron. Soc. Japan **63**(sp2), S605–S612 (2011).
24. P. S. Nugraha, G. Krizsán, and G. Polónyi, "Efficient semiconductor multicycle terahertz pulse source," J. Phys. B: At. Mol. Opt. Phys. **51**(9), 094007 (2018).
25. D. Nelson and E. Turner, "Electro-optic and piezoelectric coefficients and refractive index of Gallium Phosphide," J. Appl. Phys. **39**(7), 3337–3343 (1968).
26. Y.-S. Lee, *Principles of Terahertz Science and Technology* (Springer Science & Business Media, 2009) Chap. 3.3.2.